Received: 21 January 2021 | Revised: 3 April 2021 | Accepted: 13 April 2021

DOI: 10.1111/cas.14917

ORIGINAL ARTICLE

Cancer Science WILEY

Methylation of NRN1 is a novel synthetic lethal marker of PI3K-Akt-mTOR and ATR inhibitors in esophageal cancer

Wushuang Du[1,2] | Aiai Gao[2] | James G. Herman[3] | Lidong Wang[4] | Lirong Zhang[4] | Shunchang Jiao[1,5] | Mingzhou Guo[2,4,6]

[1]Department of Oncology, Chinese PLA General Hospital, Beijing, China

[2]Department of Gastroenterology & Hepatology, Chinese PLA General Hospital, Beijing, China

[3]UPMC Hillman Cancer Center, University of Pittsburgh, Pittsburgh, Pennsylvania, USA

[4]Henan Key Laboratory for Esophageal Cancer Research, Zhengzhou University, Zhengzhou, China

[5]Beijing Key Laboratory of Cell Engineering & Antibody, Beijing, China

[6]State Key Laboratory of Kidney Diseases, Chinese PLA General Hospital, Beijing, China

Correspondence
Mingzhou Guo, Department of Gastroenterology & Hepatology, Chinese PLA General Hospital, #28 Fuxing Road, Beijing 100853, China.
Email: mzguo@hotmail.com

Shunchang Jiao, Department of Oncology, Chinese PLA General Hospital, #28 Fuxing Road, Beijing 100853, China.
Email: jiaosc@vip.sina.com

Funding information
National Key Research and Development Program of China, Grant/Award Number: 2018YFA0208902 and 2020YFC2002705; National Science Foundation of China, Grant/Award Number: U1604281 and 81672138; Beijing Science Foundation of China, Grant/Award Number: BJSFC No. 7171008; National Key Scientific Instrument Special Program of China, Grant/Award Number: 2011YQ03013405

Abstract

Wnt, PI3K-Akt-mTOR, and NF-κB pathways were reported to be involved in DNA damage repair (DDR). DDR-deficient cancers become critically dependent on backup DNA repair pathways. Neuritin 1 (NRN1) is reported to be involved in PI3K-Akt-mTOR, and its role in DDR remains unclear. Methylation-specific PCR, siRNA, flow cytometry, esophageal cancer cell lines, and xenograft mouse models were used to examine the role of NRN1 in esophageal cancer. The expression of NRN1 is frequently repressed by promoter region methylation in human esophageal cancer cells. NRN1 was methylated in 50.4% (510/1012) of primary esophageal cancer samples. NRN1 methylation is associated significantly with age ($P < .001$), tumor size ($P < .01$), TNM stage ($P < .001$), differentiation ($P < .001$) and alcohol consumption ($P < .05$). We found that NRN1 methylation is an independent prognostic factor for poor 5-y overall survival ($P < .001$). NRN1 inhibits colony formation, cell proliferation, migration, and invasion, and induces apoptosis and G1/S arrest in esophageal cancer cells. NRN1 suppresses KYSE150 and KYSE30 cells xenografts growth in nude mice. PI3K signaling is reported to activate ATR signaling by targeting CHK1, the downstream component of ATR. By analyzing the synthetic efficiency of NVP-BEZ235 (PI3K inhibitor) and VE-822 (an ATR inhibitor), we found that the combination of NVP-BEZ235 and VE-822 increased cytotoxicity in NRN1 methylated esophageal cancer cells, as well as KYSE150 cell xenografts. In conclusion, NRN1 suppresses esophageal cancer growth both in vitro and in vivo by inhibiting PI3K-Akt-mTOR signaling. Methylation of NRN1 is a novel synthetic lethal marker for PI3K-Akt-mTOR and ATR inhibitors in human esophageal cancer.

KEYWORDS
ATR inhibitor, DNA damage repair, DNA methylation, NRN1, PI3K signaling

Wushuang Du and Aiai Gao contributed equally to this work.

1 | INTRODUCTION

Esophageal cancer (EC) is the 7th most frequently malignancy and ranks the 6th cause of cancer-related deaths.[1] Population-based studies have shown an improvement in the overall 5-y survival from less than 5% in the 1960s to *c*. 20% in the past decade in some European countries, the USA, and China.[2,3] Esophageal squamous cell carcinoma (ESCC) and esophageal adenocarcinoma (EAC) are 2 histological subtypes of EC, with ESCC accounting for 90% of cases worldwide.[4] The so-called "Asian esophageal cancer belt," extending from northern Iran through central China, represents a particularly high-risk area for ESCC, with China alone accounting for more than half of global cases.[5] The main risk factors for ESCC are tobacco smoking (including swallowed toxins from cigarette smoke) and alcohol over consumption, particularly when in combination.[6] For patients with advanced and metastatic disease, systemic therapy constitutes the primary treatment modality, with combination chemotherapy the standard treatment.[7] However, in addition to traditional cytotoxic agents, the 1st targeted therapy to gain approval in gastroesophageal cancer was the anti-HER2 monoclonal antibody trastuzumab (Herceptin).[8] This demonstrated the value of understanding the molecular changes that drive EC pathway assessment using comprehensive genomic analyses that suggested that somatic aberrations alter Notch, Wnt, and cell cycle signaling, all crucial oncogenic pathways.[9,10] Epigenetic changes link the genome, development, and environmental exposure,[11] with changes in DNA methylation most commonly studied in human disease, as it is stable and easily measured. Aberrant DNA methylation has been reported in many of the genes involved in cell cycle, DNA damage repair (DDR), Wnt, PI3K-Akt-mTOR, and NF-κB pathways.[5] DDR defects can be targeted in cancer therapy, as DDR-deficient cancers are critically dependent on salvage DNA repair pathways.[12] As BRCA1 and BRCA2 proteins are critical for the repair of double-stranded breaks (DSBs) by homology recombination repair (HR), the synthetic lethal interaction between PARP inhibition and BRCA1 or BRCA2 mutation led Farmer and Bryant to develop a novel treatment strategy for BRCA-mutant tumors.[13] With the greater understanding of DDR, additional small molecules are being developed as new anticancer therapies targeting DDR.[12] The focus of this study was an assessment of alterations of DNA methylation at loci that control these key oncogenic pathways that might potentially identify new therapeutic strategies.

The neurotrophic proteins (NTs) family is an important factor in promoting angiogenesis, neuronal differentiation and function, and also cell proliferation and apoptosis.[14,15] Neuritin 1 (NRN1), also known as the candidate plasticity-related gene (CPG15), is a member of the NTs family.[16] NRN1 plays a crucial role in apoptosis, neuronal network reconstruction, and maintenance, axonal regeneration, and possibly in tumorigenesis and nerve development.[17] Neuritin 1 (NRN1) is reported to be involved in PI3K-Akt-mTOR.[18,19] Wnt, PI3K-Akt-mTOR, and NF-κB pathways have been reported to be involved in DDR.[18,20] NRN1 was reported to be highly expressed in astrocytomas, gastric cancer, and melanoma,[21-23] while expression of NRN1 was downregulated in bladder urothelial carcinoma, breast invasive carcinoma, colon adenocarcinoma, and other cancers by analysis of The Cancer Genome Atlas (TCGA) database. NRN1 has altered DNA methylation in breast, pancreatic, and ovarian cancers.[24-28] The expression and function of NRN1 in human EC remain unclear. In this study, we analyzed the epigenetic regulation of NRN1 in human EC, and the relationship of this alteration to DNA damage repair and oncogenic signaling to determine if changes in this gene could guide a targeted therapeutic strategy.

2 | MATERIALS AND METHODS

2.1 | Human tissue samples and cell lines

In total, 1012 cases of ESCC and 15 cases of normal esophageal mucosa were collected from the Chinese PLA General Hospital. The median age of the patients with cancer was 62.5 y old (range 37-89 y), and the ratio of men:women was 3:1. All cancer samples were classified in accordance with TNM staging (AJCC 2019), including 73 cases of stage I, 438 cases of stage II, 276 cases of stage III and 225 cases of stage IV. All samples were collected from patients without chemo-radiotherapy before surgery. Sample collection was performed following the guidelines approved by the Institutional Review Board of the Chinese PLA General Hospital with written informed consent from patients.

Eight EC cell lines (KYSE30, KYSE70, KYSE140, KESE150, KYSE180, KYSE410, KYSE450, and KYSE510) were previously established from primary EC and cultured in 90% RPMI 1640 medium (Invitrogen) supplemented with 10% fetal bovine serum and 1% penicillin/streptomycin solution (Sigma).

2.2 | 5-Aza-2′-deoxycytidine treatment

For methylation regulation analysis, EC cell lines were split to a low density (30% confluence) 12 h before treatment. Cells were treated with 5-aza-2′-deoxycytidine (5-aza; Sigma) at a concentration of 2 μM. Growth medium conditioned with 5-aza at a concentration of 2 μM was exchanged every 24 h for 96 h of treatment.

2.3 | RNA isolation and semi-quantitative reverse transcription PCR

Total RNA was isolated using TRIzol reagent (Life Technologies). Agarose gel electrophoresis and spectrophotometric analysis were used to detect RNA quality and quantity. First-strand cDNA was synthesized in accordance with the manufacturer's instructions (Invitrogen). PCR primers for NRN1 are 5′-TCCCCCGCGTTCTCTAAACT-3′ (F) and

5′-GCCCAGCTTGAGCAAACAGT-3′ (R). The primer sets for NRN1 were designed to span intronic sequences between adjacent exons to control for genomic DNA contamination. Semi-quantitative reverse transcription PCR (RT-PCR) was amplified for 35 cycles. GAPDH was amplified for 25 cycles as an internal control. GAPDH primer sequences were as follows: 5′-GACCACAGTCCATGCCATCAC-3′ (F) and 5′-GTCCACCACCCTGTTGCTGTA-3′ (R). The amplified PCR products were examined using 2% agarose gels.

2.4 | DNA extraction, bisulfite modification, methylation-specific PCR, and bisulfite sequencing

DNA was prepared using the proteinase K method. Bisulfite treatment was carried out as previously described.[29,30] Methylation-specific PCR (MSP) primers were designed in accordance with genomic sequences around transcriptional start sites (TSS) and synthesized to detect unmethylated (U) and methylated (M) alleles. Bisulfite sequencing (BSSQ) was performed as previously described.[31] BSSQ products were amplified by primers flanking the targeted the CpG islands promoter regions. The MSP primers were as follows: NRN1-M-Forward 5′-GTTGCGTGTTTACGCGTTTTAGGTTGC-3′ and NRN1-M-Reverse 5′-ACTCGATTAATTCGAAAACGCTCCTCG-3′; NRN1-U-Forward 5′-GGGTTGTGTGTTTATGTGTTTTAGGTTGT-3′ and NRN1-U-Reverse 5′-CTAACTCAATTAATTCAAAAACACTCCTCA-3′. The bisulfite sequencing primers were 5′-TTGTGTGYGGGYGGGTATG-3′ (F) and 5′-AATCCAACCCRCTCTCTACRATAC-3′ (R).

2.5 | Plasmid construction

Human full-length NRN1 CDS (GenBank accession number NM_001278710.2) was amplified and subcloned as described previously.[32] The primers used were 5′-CGCGGATCCATGGGACTTAAGTTGAACGGC-3′ (F) and 5′-CCGCTCGAGTCAGAAGGAAAGCCAGGTCG-3′ (R). NRN1 expressing lentiviral or empty vectors were packaged using the ViraPower™ lentiviral expression system (Invitrogen). Lentivirus was added to the growing medium of KYSE30 and KYSE150 cells, and NRN1 stably expressed cells were selected using blasticidin (Invitrogen) at a concentration of 2 μg/mL (KYSE30) and 4 μg/mL (KYSE150) for 2 wk.

2.6 | Cell viability detection

Cells were plated into 96-well plates at 2×10^3 cells/well, and the cell viability was measured using an MTT assay (KeyGEN Biotech) at 0, 24, 48, 72 and 96 h. Absorbance was measured on a microplate reader (Thermo Multiskan MK3) at a wavelength of 490 nm.

The IC_{50} value was detected by the MTT assay. KYSE150 cells were seeded into 96-well plates at 1500 cells/well, before or after re-expression of NRN1. Cells were treated with NVP-BES235 for 24 h at 0, 2, 4, 8, 16, 32, 64, 128 or 256 nm/L. Each experiment was repeated 3 times.

2.7 | Colony formation assay

Cell lines without NRN1 expression and cells with stably expressed NRN1were seeded at 800 cells per well in 6-well culture plates in triplicate. The complete growth medium conditioned with blasticidin at 2 μg/mL was exchanged every 72 h. After 2 wk, cells were fixed with 75% ethanol for 30 min and stained with 0.2% crystal violet (Beyotime) for visualization and counting.

2.8 | Flow cytometry

NRN1 unexpressed and re-expressed KYSE30 and KYSE150 cells, and KYSE450 with or without NRN1 knockdown were starved for 12 h for synchronization, and the cells were re-stimulated with 10% FBS for 24 h. Cells were fixed with 70% ethanol and treated using the Cell Cycle Detection Kit (KeyGen Biotech). The cells were then sorted using a FACS Caliber flow cytometer (BD Biosciences). The cell phase distribution was analyzed using the ModFitLT software (Verity Software House).

2.9 | Transwell assay

NRN1 unexpressed and re-expressed KYSE30 (3×10^4) and KYSE150 (10^5) cells, KYSE450 (10^5) with or without knockdown of NRN1 were suspended in serum-free medium and placed into the upper chamber of an 8 μm pore size transwell apparatus (Corning) and incubated for 23 h. Cells that migrated to the lower surface of the membrane were stained with crystal violet and counted in 3 independent high-power fields (×200 magnification). For invasion analysis, NRN1 unexpressed and re-expressed KYSE30 (5×10^4) and KYSE150 cells (2×10^5), KYSE450 (2×10^5) with or without knockdown of NRN1 were seeded into the upper chamber of a transwell apparatus coated with extracellular matrix gel (ECM gel; BD Biosciences) and incubated for 36 h. Cells that invaded into the lower membrane surface were stained with crystal violet and counted in 3 independent high-power fields (×200 magnification).

2.10 | siRNA knockdown technique

Selected siRNAs targeting NRN1 and the RNAi negative control duplex were used in this study. The sequences of the siRNAs targeting NRN1 and the RNAi negative control are as follows: NRN1-F: 5′-CCUUACGGAUUGCCAGGAATT-3′, NRN1-R: 5′-UUCCUGGCA AUCCGUAAGGTT-3′, Negative Control-F: 5′-UUCUCCGAACGUGUCACG UTT-3′ and Negative Control-R:

5′-ACGUGACACGUUCGGAGAATT-3′. The RNAi oligonucleotide and RNAi negative control duplex were transfected into KYSE450 cells, which expressed high levels of NRN1.

2.11 | Western blot

Protein samples from EC cells were collected and western blotting was performed as described previously.[33] Antibodies were diluted in accordance with manufacturer's instructions. The primary antibodies used were as follows: NRN1 (Abcam, CO), MMP2, MMP7, MMP9 (Bioworld Technology), cyclin A2, cyclin D1, cyclin E (Proteintech), caspase3, cleaved caspase3, Bcl-2 (Cell Signaling Technology), mTOR, p-mTOR (ZhengNeng), PI3K, AKT, p-AKT (Proteintech), ERK (Proteintech), p-ERK (Proteintech), p-histone H2aX (Santa Cruz Biotechnology), ATR (ZhengNeng), p-ATR (ZhengNeng), CHK1 (ZhengNeng), p-CHK1 (ZhengNeng), and β-actin (Beyotime Biotech).

2.12 | Immunohistochemistry

Immunohistochemistry (IHC) was performed in human EC samples and paired adjacent tissue samples. The NRN1 antibody (Abcam, CO), p-mTOR antibody (ZhengNeng), PI3K antibody (Proteintech) and p-AKT antibody (Proteintech) were diluted to 1:200, 1:200, 1:400, and 1:200, respectively. For antigen retrieval, the slides were placed in citrate antigen-repairing solution and heated in a high-pressure cooker until steam arose. The slides were kept inside the cooker for 150 s, and then cooled off at room temperature for 15 min. The staining intensity and extent of the staining area were scored using the German semi-quantitative scoring system, as described previously.[34,35]

2.13 | Xenograft mouse model

NRN1 stably expressed and unexpressed KYSE150 cells (6×10^6 cells in 0.2 mL phosphate-buffered saline) and KYSE30 cells (4×10^6 cells in 0.2 mL phosphate-buffered saline) were subcutaneously injected into the dorsal flank of 5-wk-old female BALB/c nude mice. The tumor size was measured every 3 d for 18 d beginning at 3 d after implantation. The tumor volumes were calculated in accordance with the following formula: $V = L \times W^2/2$, where V, volume (mm^3); L, biggest diameter (mm); W, smallest diameter (mm).

KYSE150 cell xenograft mice were divided into control group (2 mg/kg cisplatin dissolved in 0.9% normal saline), NVP-BEZ235 group (2 mg/kg cisplatin, 5 mg/kg NVP-BEZ235 dissolved in 10% NMP and 90% PEG300), VE-822 group (2 mg/kg cisplatin, 30 mg/kg VE822 dissolved in 5% DMSO and 45% PEG300 and 50% ddH_2O), combination group (2 mg/kg cisplatin, 5 mg/kg NVP-BEZ235 and 30 mg/kg VE822). Cisplatin was administrated intraperitoneally at day 1 and day 6. NVP-BEZ235 and VE-822 was administrated by oral gavage at days 3 and 8.

2.14 | Statistical analysis

SPSS 22.0 software (IBM) was used for data analysis. All data were presented as means ± standard deviation (SD) and analyzed using Student t test. Chi-square test and Fisher exact test were used to analyze the association of NRN1 methylation status with clinicopathologic factors and the association of NRN1 expression with methylation status. Kaplan-Meier plots and the log-rank test were used to estimate the effect of 2 experimental groups in overall survival (OS). The association of risk factors (gender, age, tumor size, differentiation, lymph node metastasis, NRN1 expression, smoking, alcohol consumption, and family history) with OS was assessed by univariate and multivariate Cox proportional hazards regression models. The value of $P < .05$ is statistically significant.

3 | RESULTS

3.1 | NRN1 expression is regulated by promoter region methylation in ESCC cell lines

NRN1 expression was detected by semi-quantitative RT-PCR in human EC cell lines. As shown in Figure 1A, complete loss of NRN1 expression was found in KYSE30, KYSE150 cells. and KYSE510 cells, and reduced NRN1 expression was found in KYSE410 cells. High-level expression of NRN1 was detected in KYSE70, KYSE140, KYSE180, and KYSE450. DNA methylation of the NRN1 promoter was examined by MSP (Figure 1B). Complete methylation was found in KYSE30, KYSE150, and KYSE510 cells, cell lines with complete loss of expression. In contrast, the NRN1 promoter region was completely unmethylated in KYSE70, KYSE140, KYSE180, and KYSE450 cells, all having high levels of NRN1 expression. Partial methylation was found in KYSE410 cells, where low-level expression occurred. These results correlated the loss of expression or reduced expression of NRN1 with promoter region DNA methylation in human EC cells. To further examine the methylation density and confirm the MSP results, bisulfite sequencing was used. As shown in Figure 1C, NRN1 was completely methylated in KYSE30 and KYSE150 cells, partially methylated in KYSE410 cells, and unmethylated in KYSE450 cells, all consistent with MSP findings. To further determine whether NRN1 expression is silenced by promoter region methylation, KYSE30, KYSE70, KYSE140, KYSE150, KYSE180, KYSE410, KYSE450, and KYSE510 cells were treated with 5-aza, a demethylating reagent. Restoration of NRN1 expression was induced by 5-aza in KYSE30, KYSE150 KYSE410, and KYSE510 cells, all harboring promoter region methylation, while no expression changes were found in KYSE70, KYSE140, KYSE180, and KYSE450 cells, all unmethylated at baseline, before and after 5-aza treatment (Figure 1A). Collectively, these results

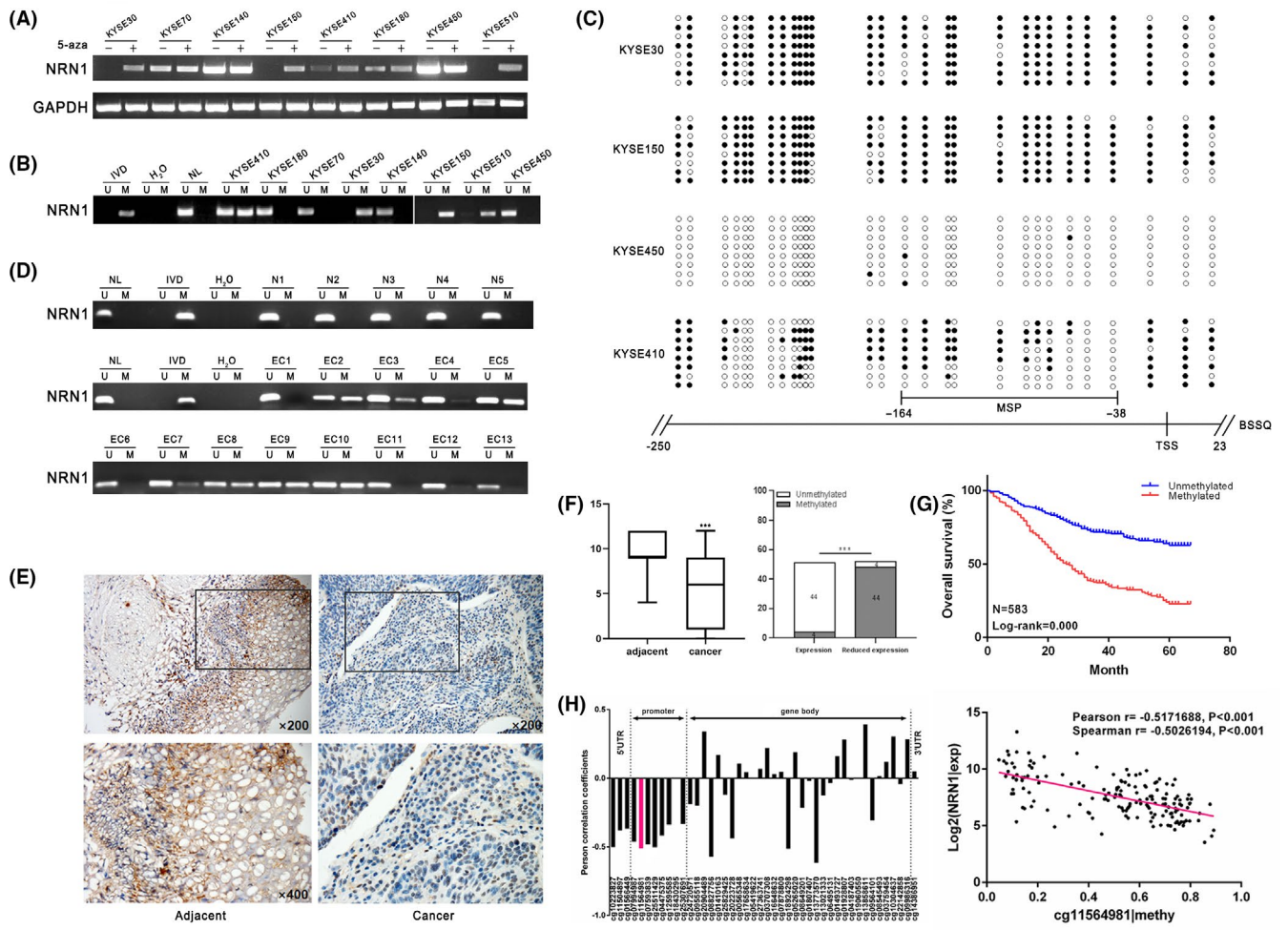

FIGURE 1 NRN1 expression and methylation status in human ESCC cells. A, Semi-quantitative RT-PCR shows NRN1 expression levels in esophageal cancer (EC) cell lines. KYSE30, KYSE70, KYSE140, KYSE150, KYSE180, KYSE410, KYSE450, and KYSE510 are ESCCs. 5-aza: 5-aza-2′-deoxycytidine; GAPDH: internal control; (−): absence of 5-aza; (+): presence of 5-aza. B, MSP results of NRN1 in ESCCs. U: unmethylated alleles; M: methylated alleles; IVD: in vitro methylated DNA, serves as methylation control; NL: normal peripheral lymphocytes DNA, serves as unmethylated control; H_2O: double-distilled water. C, BSSQ results of NRN1 in KYSE30, KYSE150, KYSE450, and KYSE410 cells. MSP PCR product size was 126 bp and bisulfite sequencing focused on a 278-bp region of the CpG islands (from −250 to 23) around the NRN1 transcription start site. Filled circles: methylated CpG sites, open circles: unmethylated CpG sites. TSS: transcription start site. D, Representative MSP results of NRN1 in normal esophageal mucosa samples and primary EC samples. N: normal esophageal mucosa samples; EC: primary esophageal cancer samples. E, Representative IHC results show NRN1 expression in EC tissue and adjacent tissue samples (top: ×200 magnification; bottom: ×400 magnification). F, NRN1 expression scores are shown as box plots, horizontal lines represent the median score; the bottom and top of the boxes represent the 25th and 75th percentiles, respectively; vertical bars represent the range of data. Expression of NRN1 was significantly different between adjacent tissue and EC tissue in 96-matched EC samples. ***$P < .001$. G, NRN1 methylation status is associated with OS of ESCC patients. H, Pearson correlation coefficient between NRN1 methylation and expression at each CpG site. TSS: transcription start site. Scatter plots showing the methylation status of the 7th (cg11564981) CpG sites, which are correlated with loss or reduced NRN1 expression. β-value were considered methylated. ***$P < .001$

showed that expression of NRN1 was repressed by promoter region methylation in a subset of human ECs.

3.2 | NRN1 is frequently methylated in primary human ESCC

To examine whether methylation of NRN1 was prevalent in primary human EC, DNA methylation was examined by MSP in 1012 cases of EC tissue samples and 15 cases of normal esophageal mucosa from non-cancerous patients. NRN1 was methylated in 50.4% (510/1012) of primary EC samples, while no methylation was detected in 15 normal esophageal mucosa samples (Figure 1D). As shown in Table 1, NRN1 methylation was associated significantly with age ($P < .001$), tumor size ($P < .01$), TNM stage ($P < .001$), differentiation ($P < .001$) and alcohol consumption ($P < .05$), but no association was found between NRN1 methylation and gender, lymph node metastasis or smoking (all $P > .05$).

For 583 cases of this cohort where OS data were available, a Cox proportional hazards model was used to assess the association of

TABLE 1 Clinical factors and NRN1 methylation in 1012 cases of esophageal cancer

Clinical factor	No.	NRN1 methylation status		*P*-value*
		Methylated *n* = 510 (50.4%)	Unmethylated *n* = 502 (49.6%)	
Age (y)				
<60	283	108	175	$P = .0000^{***}$
≥60	729	402	327	
Gender				
Male	667	341	326	$P = .5189$
Female	345	169	176	
Tumor size (cm)				
<4	443	201	242	$P = .0048^{**}$
≥4	569	309	260	
Differentiation				
Well + Moderate	471	132	339	$P = .0000^{***}$
Poor	541	378	163	
TNM stage				
I + II	535	209	326	$P = .0000^{***}$
III + IV	477	301	176	
Lymph node Metastasis				
N0	502	241	261	$P = .1318$
N1	510	269	241	
Smoking				$P = .6915$
Yes	564	273	275	
No	457	237	227	
Alcohol consumption				$P = .0213^{*}$
Yes	401	220	181	
No	611	290	321	

*$P < .05$; **$P < .01$; ***$P < .001$.

NRN1 methylation with survival. As shown in Figure 1G and Table 2, NRN1 methylation is an independent prognostic factor for poor 5-y OS ($P < .001$).

To analyze the association of NRN1 expression and methylation, 96 cases of available matched EC and adjacent tissue paraffin samples were evaluated by IHC. As shown in Figure 1E,F, NRN1 expression is mainly detected in the cytoplasm. NRN1 is highly expressed in adjacent tissue samples and generally reduced in primary cancer tissue samples. However, when expression of NRN1 was compared with NRN1 promoter region methylation, we found a strong inverse relationship with expression, DNA methylation was found in 44 of 48 tumors with reduced expression, while only 4 of 48 tumors that retained expression had detectable NRN1 methylation ($P < .01$). The results further suggest that expression of NRN1 is reduced by promoter region methylation in approximately 50% of primary EC.

Our finding of frequent methylation of NRN1 in EC was confirmed by examining TCGA database. As shown in Figure 1H, multiple probes in the 5′UTR and promoter region have increased methylation with an inverse correlation to gene expression. This inverse association is shown in detail for 1 promoter region probe (cg11564981), where increase level of methylation (increase in beta value) is associated with loss/reduced expression of NRN1 in 162 cases of ECs (Figure 1H, Pearson $r = -0.5171688$, $P < .001$, Spearman: rho = −0.5026194, $P < .001$).

3.3 | Restoration of NRN1 expression induces ESCC cell apoptosis

Flow cytometry was used to assess the effect of NRN1 on apoptosis. The percentage of apoptotic cells increased with NRN1 expression in cell lines with baseline NRN1 silencing, from 1.433 ± 0.23% to 7.867 ± 0.11% ($P < .001$) in KYSE150 cells, and from 2.0 ± 0.2% to 7.93 ± 0.11% ($P < .001$) in KYSE30 cells (Figure 2A). The KYSE450 knockdown of NRN1 decreased the percentage of apoptotic cells from 11.67 ± 0.71% to 2.8 ± 0.3% (Figure 2A, $P < .001$). To further characterize the effect of NRN1 on apoptosis, expression of caspase-3, cleaved caspase-3, and Bcl-2 were detected by western blot. As shown in Figure 2G, the levels of caspase-3 and Bcl-2 were decreased and the levels of cleaved caspase-3 were

TABLE 2 Univariate and multivariate analysis of NRN1 methylation status with overall survival in esophageal cancer patients (n = 583)

Clinical parameter	Univariate analysis		Multivariate analysis	
	HR (95%CI)	*P*-value	HR (95%CI)	*P*-value
Gender (male vs female)	0.939 (0.688-1.282)	$P = .192$		
Age (≤60 vs >60 y)	0.467 (0.104-0.949)	$P = .654$		
Tumor size (≤4 vs >4 cm)	1.355 (1.061-1.731)	$P = .014^{*}$	0.764 (0.598-0.973)	$P = .031^{*}$
Differentiation (high or middle vs low differentiation)	0.679 (0.871-1.921)	$P = .911$		
Lymph node metastasis (negative vs positive)	0.440 (0.345-0.561)	$P = .000^{***}$	0.451 (0.353-0.575)	$P = .000^{***}$
TNM	1.771	$P = .000^{***}$	1.433	$P = .018^{*}$
(I + II vs III + IV)	(1.394-2.251)		(1.064-1.932)	
NRN1 (unmethylation vs methylation)	1.317 (1.245-2.311)	$P = .000^{***}$	1.322 (1.249-2.318)	$P = .000^{***}$
Smoking (no vs yes)	1.489 (1.005-1.693)	$P = .253$		
Alcohol consumption (no vs yes)	1.329 (1.009-1.775)	$P = .048^{*}$	0.488 (0.229-0.740)	$P = .306$
Family history (no vs yes)	0.871 (0.574-1.233)	$P = .154$		

Abbreviation: HR, Hazard ratio;
$^{*}P < .05$; $^{**}P < .01$; $^{***}P < .001$.

increased after re-expression of NRN1 in KYSE30 and KYSE150 cells, and caspase-3 and Bcl-2 were increased, while cleaved caspase-3 were decreased after knockdown of NRN1 in KYSE450 cells. These results demonstrated that NRN1 expression induced apoptosis in ESCC cells.

3.4 | Restoration of NRN1 expression suppresses cell proliferation and induces G1/S arrest in ESCC cells

To evaluate the effects of NRN1 on cell proliferation, cell viability was detected by MTT and colony formation assays. The OD value was 1.04 ± 0.05 vs 0.74 ± 0.04 ($P < .05$) in KYSE150 cells and 0.68 ± 0.04 vs 0.56 ± 0.05 ($P < .01$) in KYSE30 cells before and after restoration of NRN1 expression (Figure 2B). Viability was reduced after re-expression of NRN1. The colony numbers were 127 ± 3.6 vs 90 ± 5.5 ($P < .01$) in KYSE150 cells and 181 ± 18.2 vs 109 ± 12.3 ($P < .01$) in KYSE30 cells before and after restoration of NRN1 expression (Figure 2C). These results suggested that NRN1 suppresses EC cell proliferation.

To further understand the mechanism of NRN1 in EC development, the effect of NRN1 on cell cycle was evaluated by flow cytometry. In KYSE150 cells, the cell cycle distribution before and after re-expression of NRN1 was as follows: G0/G1 phase: 33.46 ± 0.58% vs 40.82 ± 1.73% ($P < .01$), S phase: 43.17 ± 0.94% vs 39.15 ± 1.21% ($P < .05$), and G2/M phase: 23.37 ± 2.21% vs 20.03 ± 0.31%. In KYSE30 cells, the cell cycle distribution before and after re-expression of NRN1 was as follows: G0/G1 phase: 39.37 ± 1.34% vs 47.35 ± 2.54% ($P < .01$), S phase: 36.38 ± 1.65% vs 32.56 ± 0.96% ($P < .05$), and G2/M phase: 24.25 ± 1.16% vs 20.09 ± 2.36%. The G0/G1 phase increased significantly after re-expression of NRN1 (Figure 2D). The effect of NRN1 on cell cycle was further validated by knocking down NRN1 in KYSE450 cells. The cell phase distribution was as follows: G0/G1 phase: 43.45 ± 0.64% vs 36.76 ± 0.84% ($P < .01$), S phase: 47.58 ± 1.46% vs 52.56 ± 1.79% ($P < .05$) and G2/M phase: 8.96 ± 0.88% vs 10.66 ± 2.35%. The G0/G1 phase decreased significantly by knocking down NRN1 (Figure 2D). Above all results suggested that NRN1 induced G0/1 arrest. As shown in Figure 2G, the levels of cyclin A2, cyclin D1 and cyclin E were decreased in KYSE30 and KYSE150 cells when NRN1 was re-expressed, and increased in KYSE450 cell by knocking down NRN1. These results suggested that NRN1 induced G1/S arrest in EC cells.

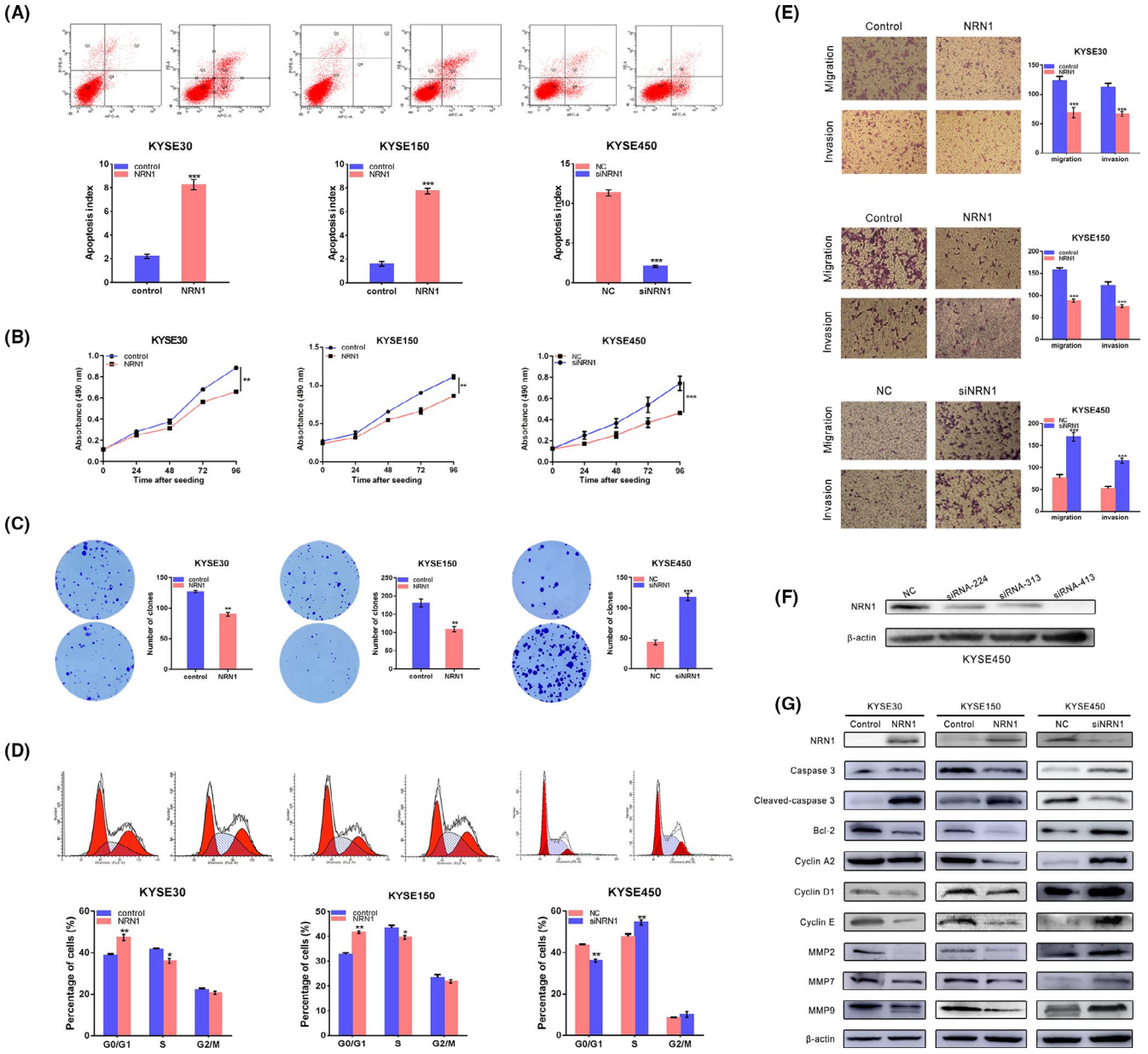

FIGURE 2 Effect of NRN1 on esophageal cancer (EC) cell proliferation, apoptosis, cell cycle, invasion, and migration. A, Flow cytometry results show induction of apoptosis by re-expression of NRN1 in KYSE30 and KYSE150 cells, while reduction of apoptosis was found after knockdown of NRN1 in KYSE450 cells. $^{**}P < .01$. B, Growth curves represent cell viability analyzed by the MTT assay in NRN1 re-expressed and unexpressed KYSE30 and KYSE150 cells, as well as in KYSE450 cell before and after knockdown of NRN1. Each experiment was repeated in triplicate. $^{**}P < .01$, $^{***}P < .001$. C, Colony formation results show that colony numbers were reduced by re-expression of NRN1 in KYSE30 and KYSE150 cells, while they were increased by knockdown of NRN1 in KYSE450 cells. Each experiment was repeated in triplicate. Average number of tumor clones is represented by bar diagram. $^{**}P < .01$, $^{***}P < .001$. D, Cell phase distribution in NRN1 unexpressed and re-expressed KYSE30 and KYSE150 cells, as well as cell phase distribution before and after knockdown of NRN1 in KYSE450 cells. Each experiment was repeated 3 times. $^{*}P < .05$, $^{**}P < .01$. E, The migration assays show migration cells before and after restoration of NRN1 expression in KYSE30 and KYSE150 cells. The invasion assays show invasive cells before and after restoration of NRN1 expression in KYSE450. $^{***}P < .001$. F, Western blots show the effects of knockdown of NRN1 by different siRNA. NC: siRNA negative control; siNRN1: siRNA for NRN1. G, Western blots show the effects of NRN1 on the levels of caspase-3, cleaved caspase-3, Bcl-2, cyclinA2, cyclinD1, cyclin E, MMP2, MMP7, and MMP9 expression in KYSE30, KYSE150, and KYSE450 cells. GFP: control vector, NRN1: NRN1 expressing vector, β-actin: internal control. NC: siRNA negative control; siNRN1: siRNA for NRN1

3.5 | Restoration of NRN1 expression inhibits cell migration and invasion in ESCC cells

The effect of NRN1 on cell migration was evaluated by transwell assay. The number of migrated cells for each high-power field under the microscope was 158.1 ± 18.3 vs 90.7 ± 19.0 in KYSE150 cells and 119.4 ± 29.0 vs 68.0 ± 24.2 in KYSE30 cells before and after restoration of NRN1 expression. The number of migratory cells was 77.7 ± 5.2 vs 163.0 ± 5.3 before and after knockdown of NRN1 in KYSE450 cells. The cell number was reduced significantly after

re-expression of NRN1 in EC cells (all $P < .001$, Figure 2E). These results demonstrated that NRN1 inhibits ESCC cell migration. The number of invasive cells for each high-power field under the microscope was 129.7 ± 11.7 vs 78.7 ± 6.2 in KYSE30 cells and 116.1 ± 9.1 vs 68.4 ± 8.9 in KYSE150 cells before and after restoration of NRN1 expression. The cell number was reduced significantly after re-expression of NRN1 in KYSE30 and KYSE150 cells (all $P < .001$, Figure 2E). The number of invasive cells was 57.3 ± 6.7 vs 115.3 ± 8.5 before and after knockdown of NRN1 in KYSE450 cells ($P < .001$, Figure 2E). These results suggested that NRN1 inhibits ESCC cell invasion.

To further understand the mechanism of NRN1 in ESCC migration and invasion, the expression levels of MMP2, MMP7, and MMP9 were detected by western blot. The levels of MMP2, MMP7, and MMP9 were reduced after re-expression of NRN1 in KYSE30 and KYSE150 cells. The inhibitory role of NRN1 on MMP2, MMP7, and MMP9 expression was further validated by knocking down NRN1 in KYSE450 cells (Figure 2G). The above results suggested that NRN1 suppresses EC cell migration and invasion.

3.6 | NRN1 suppresses ESCC cell xenograft growth in nude mice

To explore the effect of NRN1 on EC in vivo, NRN1 unexpressed and re-expressed KYSE150 and KYSE30 cells xenograft mouse models were used (Figure 3A). The tumor volume was 269.4 ± 70.7 mm^3 in NRN1 unexpressed KYSE30 xenografts and 137.2 ± 52.3 mm^3 in NRN1 re-expressed KYSE30 xenografts ($P < .001$). The tumor volume was 378.4 ± 59.1 mm^3 in NRN1 unexpressed KYSE150 xenografts and 167.3 ± 31.5 mm^3 in NRN1 re-expressed KYSE150 xenografts ($P < .01$). The volume is smaller in NRN1 re-expressed xenografts compared with NRN1 unexpressed xenografts (Figure 3B). The tumor weight was 162.2 ± 10.1 mg in NRN1 unexpressed xenografts and 26.0 ± 10.7 mg in NRN1 re-expressed KYSE30 xenografts. In KYSE150 xenografts, the tumor weight was 102.2 ± 11.9 mg in NRN unexpressed group and 49.0 ± 8.9 in NRN1 re-expressed group. The tumor weight is lower in NRN1 expressed xenografts compared with NRN1 unexpressed xenografts (both $P < .001$, Figure 3C).

3.7 | NRN1 inhibits PI3K-Akt-mTOR signaling in ESCC cells

NRN1 has been reported to regulate ERK/mTOR signaling in the development of cerebellar granule neurons.[18] To determine whether NRN1 regulates this pathway in EC, the levels of PI3K, AKT, p-AKT, mTOR, p-mTOR, ERK, and p-ERK were examined before and after re-expression of NRN1 in KYSE30 and KYSE150 cells. As shown in Figure 3E, expression of PI3K, p-AKT, and p-mTOR were decreased when NRN1 was expressed in these cell lines with basally silenced NRN1, but no changes were found in AKT, mTOR, and ERK expression, or levels of p-ERK after re-expression of NRN1. Concordant increases in the levels of PI3K, p-AKT, and p-mTOR with knockdown of NRN1 were seen in KYSE450 cells. These studies demonstrated that PI3K-Akt-mTOR signaling is normally inhibited by NRN1 in EC cells, with pathway activation present with NRN1 loss of expression, while ERK signaling is not affected.

The effect of NRN1 on PI3K-Akt-mTOR signaling was also evaluated by staining p-mTOR, PI3K, and p-AKT in the previously studied xenografts using IHC. Staining of p-mTOR, PI3K, and p-AKT was reduced with restored NRN1 expression (Figure 3D) in these xenografts, further demonstrating the importance of NRN1 inhibition of PI3K-mTOR signaling in ESCC.

To further validate the similar effect of NRN1 and PI3K-Akt-mTOR inhibitor, NVP-BEZ235, a PI3K-Akt-mTOR inhibitor, was used. The levels of PI3K, p-AKT, and p-mTOR were reduced after NVP-BEZ235 treatment in NRN1 unexpressed KYSE150 cells, while no apparent changes were found in NRN1 stably expressed KYSE150 cells before and after NVP-BEZ235 treatment (Figure 3F). The results further suggested that NRN1 inhibits PI3K-Akt-mTOR signaling in ESCC.

3.8 | Methylation of NRN1 is a sensitive marker for combined PI3K-Akt-mTOR inhibitor and ATR inhibitor treatment

PI3K-Akt-mTOR signaling is important in maintaining genomic stability by involving DNA replication and cell cycle regulation.[20] PI3K inhibition causes genomic instability and mitotic catastrophe, and also increases replication stress and subsequent DNA damage.[12,36,37] In ovarian cancer, compared with monotherapy, combined samotolisib (PI3K/mTOR inhibitor) and prexasertib (CHK1 inhibitor) treatment increased DNA damage, suggesting that PI3K/mTOR inhibitor augmented CHK1 inhibitor-induced DNA damage.[38] Another study suggests that combined inhibition of mTOR and ATR or Chk1 increased the efficiency in breast cancer, because all these pathways needed an S phase.[39] Our study found that silencing of NRN1 by DNA methylation activated PI3K-Akt-mTOR signaling in ESCC. Therefore, we explored the synthetic efficiency of NVP-BEZ235 (PI3K inhibitor) and VE-822 (an ATR inhibitor) in NRN1 silenced KYSE30 and KYSE150 cells. Cytotoxicity was evaluated by MTT assay. The OD values were 0.723 ± 0.02 and 0.466 ± 0.02 for VE-822 and combined NVP-BEZ235 and VE-822 treatment in KYSE30 cells ($P < .01$, Figure 4A). In KYSE150 cells, the OD values were 0.733 ± 0.04 and 0.479 ± 0.03 for VE-822 treatment and combined NVP-BEZ235 and VE-822 treatment ($P < .01$, Figure 4B). When knockdown of NRN1 in KYSE450 cells, the OD values were 0.678 ± 0.10 and 0.401 ± 0.05 for VE-822 and combined NVP-BEZ235 and VE-822 treatment. The OD value is reduced significant in combined NVP-BEZ235 and VE-822 treatment ($P < .01$, Figure 4C). The above results demonstrated that combined NVP-BEZ235 and VE-822 increased cytotoxicity in NRN1 methylated EC cells.

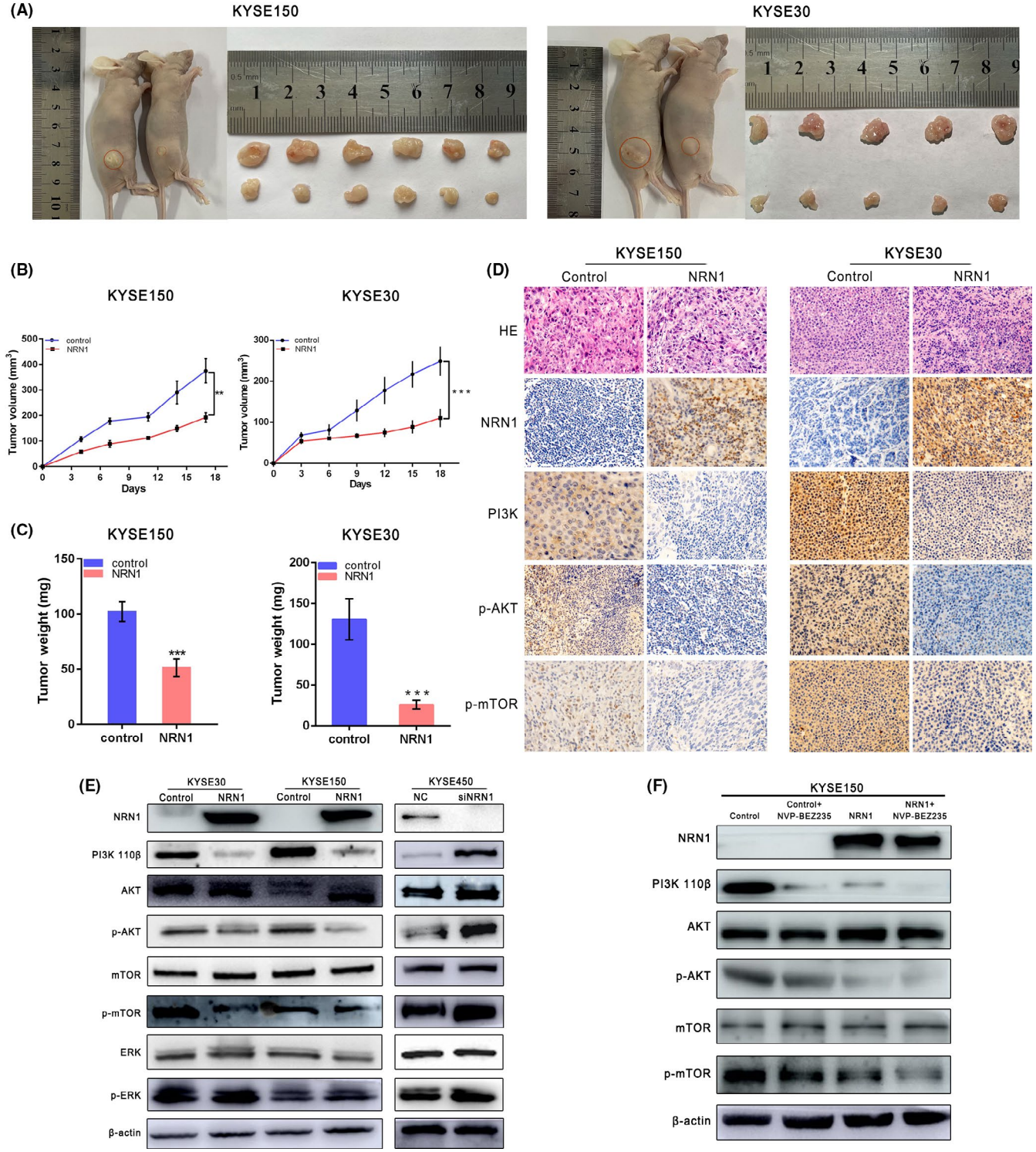

FIGURE 3 NRN1 suppresses human esophageal cancer (EC) cell xenograft growth in mice and NRN1 inhibits the PI3K-Akt-mTOR signaling pathway in vitro and in vivo. A, Representative tumors from NRN1 unexpressed and NRN1 re-expressed KYSE150 and KYSE30 cell xenografts. B, Tumor growth curves of NRN1 unexpressed and NRN1 re-expressed KYSE150 and KYSE30 cells. $^{**}P < .01$, $^{***}P < .001$. C, Tumor weights in nude mice at the 18th day after inoculation of unexpressed and NRN1 re-expressed KYSE150 and KYSE30 cells. Bars: mean of 8 mice. $^{***}P < .001$. D, Images of hematoxylin and eosin staining show tumors from NRN1 unexpressed and NRN1 re-expressed KYSE150 and KYSE30 xenograft mice. IHC staining reveals the expression levels of NRN1, PI3K, p-AKT, and p-mTOR in NRN1 unexpressed andNRN1 re-expressed KYSE150 and KYSE30 cell xenografts. E, Western blots show the levels of NRN1, PI3K, AKT, p-AKT, mTOR, p-mTOR, ERK, p-ERK, and β-actin in KYSE30, KYSE150, and KYSE450 cells. β-actin: internal control. F, Expression levels of NRN1, PI3K, AKT, p-AKT, mTOR, p-mTOR, and β-actin were detected by western blot in NRN1 unexpressed and re-expressed KYSE150 cells. NVP-BEZ235: a PI3K-Akt-mTOR inhibitor; (−): absence of NVP-BEZ235; (+): presence of NVP-BEZ235

The synthetic lethal efficiency was further validated by treatment with ATR/CHK1 inhibitor and PI3K inhibitor in NRN1 silenced KYSE30 and KYSE150 cells, as well as in KYSE450 cells by knocking down NRN1 with siRNA. DNA damaging efficiency was evaluated by detection of the levels of ATR, p-ATR, CHK1, p-CHK1, and p-H2AX. Under cisplatin treatment, the levels of p-ATR and p-CHK1 were increased apparently after treatment with NVP-BEZ235 in NRN1 silenced KYSE30 and KYSE150 cells. This result suggested that loss of NRN1 expression sensitized EC cells to PI3K inhibitor. Combined NVP-BEZ235 and VE-822/prexasertib treatment reduced the levels of p-ATR and p-CHK1 and increased the levels of p-H2AX compared with VE-822 treatment only (Figure 4D,E,G). The results suggested that PI3K inhibitor synthesized with ATR/CHK1 inhibitors in NRN1 unexpressed EC cells. Under cisplatin treatment, when knocking down NRN1 in KYSE450 cells, p-ATR and p-CHK1 levels were increased after NVP-BEZ235 treatment. p-ATR and p-CHK1 levels were reduced and the levels of p-H2AX were increased in combination with NVP-BEZ235 and VE-822 treatment, compared with VE-822 treatment only (Figure 4F). The results further demonstrated that PI3K inhibitor synthesized with ATR/CHK1 inhibitors in EC cell reduced expression of NRN1. The difference between PI3K and ATR inhibitors in NRN1 expressed EC cells was also validated. Under cisplatin treatment, no apparent changes were found for the levels of p-ATR and p-CHK1 in NRN1 re-expressed KYSE30 and KYSE150 cells, as well as NRN1 highly expressed KYSE450 cells treated with VE-822 or NVP-BEZ235, or the combination (Figure 4D-F). This result suggested that there was no apparent effect of PI3K and ATR inhibitors in NRN1 expressed cells. The above results suggested that further loss of NRN1 expression by promoter region methylation is a synthetic lethal marker for ATR/CHK1 and PI3K inhibitors in human EC.

To further validate the synthetic lethal effect of combined VE-822 and NVP-BEZ235, xenograft mouse models were used. In NRN1 unexpressed KYSE150 cell xenografts, the tumor volumes were 383 ± 29.1 mm^3 in the control group, 380 i± 33.9 mm^3 in NVP-BEZ235 group, 367 ± 29.8 mm^3 in the VE-822 group, and 119 ± 21.4 mm^3 in the combination group. The tumor volume was significantly smaller in the combination group than in other groups (all $P < .001$, Figure 4H,I). Tumors weights were 111.0 ± 15.1 mg in the control group, 94.6 ± 8.3 mg in the NVP-BEZ235 group, 93.4 ± 12.2 mg in the VE-822 group, and 28.1 ± 7.3 mg in the combination group. The tumor weight was significantly less in the combination group than in other groups (all $P < .001$, Figure 4H,J). The results suggested that NVP-BEZ235 and VE-822 synthetically suppressed esophageal cancer cell xenografts growth in vivo.

4 | DISCUSSION

Currently, most targeting therapies in cancer are directly targeted at activated oncogenes or "gain of function" genetic aberrations, including gene mutation, amplification, and fusion. However, there are very limited studies that have focused on esophageal cancer targeting therapy, most of which target epidermal growth factor receptor, and a very limited number of druggable hotspot mutations have been reported.[12,40-45] Unfortunately, not all identified mutations or aberrant expressions can be directly targeted. This "loss of function" or loss of expression by inactivating gene mutations makes it hard to restore activities pharmacologically, and less success has yet been achieved.[12,46,47] Notably, a synthetic lethality strategy allows the therapeutic exploitation of both non-druggable mutated tumor suppressor genes and directly difficult to target (hard-druggable) oncogenes, by targeting their synthetic lethality partners.[48] The vast majority of human cancers harbors both genetic and epigenetic abnormalities, with fascinating interplay between both.[47] Disruption of the "epigenetic machinery" plays an important role in cancer development. For example, tumor suppressor genes were methylated in the early stage of ESCC, and accumulation of promoter region methylation was correlated with cancer progression.[47,49] Aberrant DNA methylation is involved in the major components of the cell cycle, DNA damage repair, Wnt, TGF-beta, PI3K-Akt-mTOR, and other cancer-related signaling pathways.[5,50-53] Understanding the causative epigenetic changes of "loss of function" may lead to the development of novel therapeutic strategies in cancer.

In this study, we found that NRN1 is frequently methylated in human ESCC and that the expression of NRN1 is regulated by promoter region methylation. Methylation of NRN1 is associated significantly with age, alcohol consumption, tumor size, TNM stage, and differentiation. NRN1 methylation is an independent prognostic factor for poor 5-y OS. NRN1 inhibits EC cell proliferation, colony formation, migration, and invasion, and induces cell apoptosis and G1/S cell cycle arrest. NRN1 suppressed human EC cell xenograft growth in nude mice. These results suggested that NRN1 is a tumor suppressor in human EC. Further study found that methylation of NRN1 activated PI3K-Akt-mTOR signaling in EC cells. As such, the PI3K pathway incorporates DNA replication and cell cycle regulation, and PI3K inhibition causes genomic instability and mitotic catastrophe.[54] Another report found that the combination of mTOR inhibitor and ATR inhibitor or CHK1 inhibitor increased cytotoxicity by inducing replication stress in PI3K-activated ovarian cancer cells.[38,54] Our study found that loss of NRN1 expression by promoter region methylation sensitized EC cells to PI3K inhibitor. Further study demonstrated that PI3K inhibitor synthesized with ATR/CHK1 inhibitors in NRN1 unexpressed EC cells, while there was no synthetic effect in NRN1 expressed cells. The results were validated by KYSE150 cell xenografts. These results suggested that methylation of NRN1 is a synergistic lethal marker of PI3K inhibitor and ATR inhibitor (Figure 5).

In conclusion, NRN1 is frequently methylated in human EC and the expression of NRN1 is regulated by promoter region methylation. NRN1 methylation is an independent prognostic factor for poor 5-y OS in ESCC. NRN1 suppresses EC cell growth by inhibiting PI3K-Akt-mTOR signaling both in vitro and in vivo. Methylation of NRN1 is a novel prognostic marker of synergistic lethal therapy in combination with PI3K and ATR inhibitors.

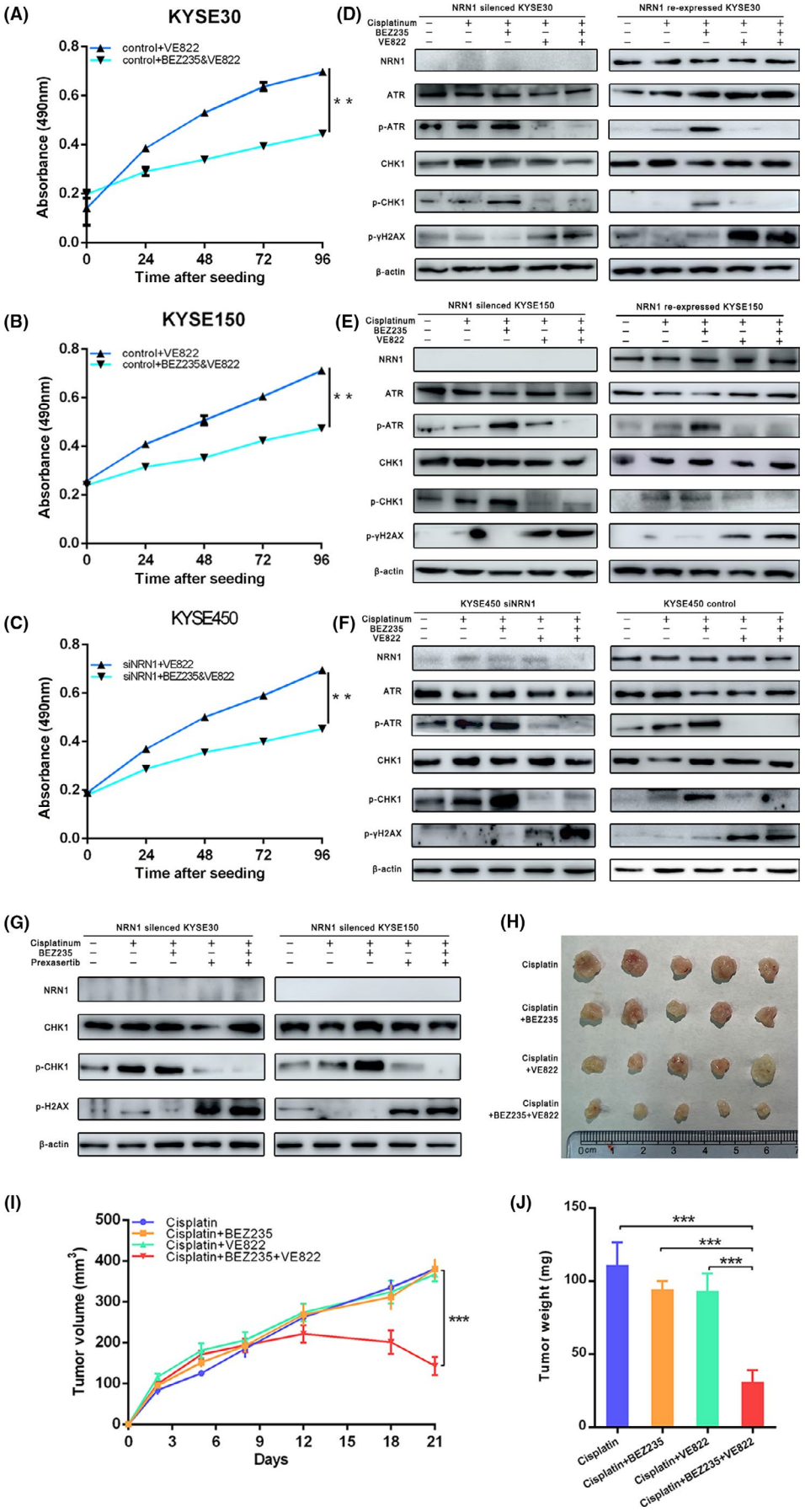
(A)
KYSE30
control+VE822
control+BEZ235&VE822
Absorbance (490nm)
Time after seeding
(B)
KYSE150
control+VE822
control+BEZ235&VE822
Absorbance (490nm)
Time after seeding
(C)
KYSE450
siNRN1+VE822
siNRN1+BEZ235&VE822
Absorbance (490nm)
Time after seeding
(D)
NRN1 silenced KYSE30
NRN1 re-expressed KYSE30
Cisplatinum
BEZ235
VE822
NRN1
ATR
p-ATR
CHK1
p-CHK1
p-γH2AX
β-actin
(E)
NRN1 silenced KYSE150
NRN1 re-expressed KYSE150
(F)
KYSE450 siNRN1
KYSE450 control
(G)
NRN1 silenced KYSE30
NRN1 silenced KYSE150
Cisplatinum
BEZ235
Prexasertib
NRN1
CHK1
p-CHK1
p-H2AX
β-actin
(H)
Cisplatin
Cisplatin +BEZ235
Cisplatin +VE822
Cisplatin +BEZ235+VE822
(I)
Cisplatin
Cisplatin+BEZ235
Cisplatin+VE822
Cisplatin+BEZ235+VE822
Tumor volume (mm3)
Days
(J)
Tumor weight (mg)
Cisplatin
Cisplatin+BEZ235
Cisplatin+VE822
Cisplatin+BEZ235+VE822

FIGURE 4 Loss of expression of NRN1 cell sensitivity to NVP-BEZ235 and VE-822 both in vitro and in vivo. A-C, Growth curves represent cell viability evaluated by MTT assay in the control group plus the VE-822 treatment and the control group plus the VE-822 and NVP-BEZ235 treatment group in NRN1 unexpressed KYSE30 and KYSE150, as well as in KYSE450 with siNRN1. VE-822: an ATR inhibitor. $^{**}P < .01$. D-F, Expression levels of NRN1, ATR, p-ATR, CHK1 and p-CHK1, γ-H2AX, and β-actin were detected by western blot in NRN1 unexpressed and re-expressed KYSE30 and KYSE150, as well as in KYSE450 cells before and after NRN1 knock down. (–) Absence of NVP-BEZ235 or VE-822 or cisplatin; (+) presence of NVP-BEZ235 or VE-822 or cisplatin. G, Expression levels of NRN1, CHK1 and p-CHK1, γ-H2AX, and β-actin were detected by western blot in NRN1 methylated KYSE30 and KYSE150 cells. (–) Absence of NVP-BEZ235 or prexasertib or cisplatin; (+) presence of NVP-BEZ235 or prexasertib or cisplatin. H, Image of tumors of 4 groups in nude mice. I, Tumor growth curves in control and treatment groups. Bars: mean of 5 mice. $^{***}P < .001$. J, Tumor weights in nude mice at the end of treatment. Bars: mean of 5 mice. $^{***}P < .001$

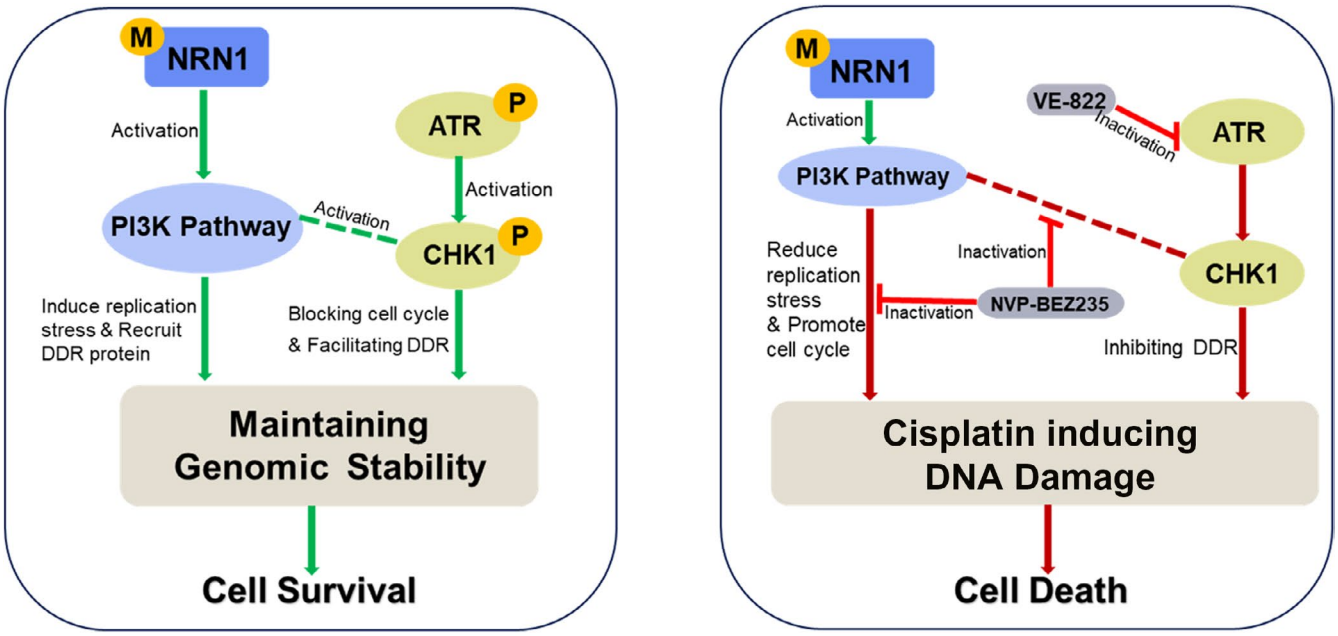

FIGURE 5 A working model of synthetic lethality for PI3K inhibitor and ATR inhibitor in NRN1 silenced cells by promoter region methylation. DDR: DNA damage repair; M: methylation; P: phosphorylation

ACKNOWLEDGMENTS

This work was supported by grants from the National Key Research and Development Program of China (2018YFA0208902, 2020YFC2002705); the National Science Foundation of China (NSFC Nos. U1604281, 81672138); Beijing Science Foundation of China (BJSFC No. 7171008); and the National Key Scientific Instrument Special Program of China (Grant No. 2011YQ03013405).

CONFLICT OF INTEREST

The authors declare no potential conflicts of interest.

ORCID

Mingzhou Guo https://orcid.org/0000-0002-9445-9984

REFERENCES

1. Bray F, Ferlay J, Soerjomataram I, Siegel RL, Torre LA, Jema A. Global cancer statistics 2018: GLOBOCAN estimates of incidence and mortality worldwide for 36 cancers in 185 countries. *CA Cancer J Clin*. 2018;68:394-424.
2. Siegel RL, Miller KD, Jemal A. Cancer statistics, 2019. *CA Cancer J Clin*. 2019;69:7-34.
3. Sun LP, Yan L-B, Liu Z-Z, et al. Dietary factors and risk of mortality among patients with esophageal cancer: a systematic review. *BMC Cancer*. 2020;20:287.
4. Ajani JA, D'Amico TA, Bentrem DJ, et al. Esophageal and esophagogastric junction cancers, version 2.2019, NCCN clinical practice guidelines in oncology. *J Natl Compr Canc Netw*. 2019;17(7):855-883.
5. Liu Y, Zhang M, He T, et al. Epigenetic silencing of IGFBPL1 promotes esophageal cancer growth by activating PI3K-AKT signaling. *Clinical Epigenetics*. 2020;12(1):22. https://doi.org/10.1186/s13148-020-0815-x
6. Prabhu A, Obi KO, Rubenstein JH. The synergistic effects of alcohol and tobacco consumption on the risk of esophageal squamous cell carcinoma: a meta-analysis. *Am J Gastroenterol*. 2014;109:822-827.
7. Wang VE, Grandis JR, Ko AH. New strategies in esophageal carcinoma: translational insights from signaling pathways and immune checkpoints. *Clin Cancer Res*. 2016;22:4283-4290.
8. Bang YJ, Van Cutsem E, Feyereislova A, et al. Trastuzumab in combination with chemotherapy versus chemotherapy alone for treatment of HER2-positive advanced gastric or gastro-oesophageal junction cancer (ToGA): a phase 3, open-label, randomised controlled trial. *Lancet*. 2010;376:687-697.
9. Lagergren J, Smyth E, Cunningham D, Lagergren P. Oesophageal cancer. *Lancet*. 2017;390:2383-2396.
10. Rustgi AK, Ingelfinger JR, El-Serag HB. Esophageal carcinoma. *N Engl J Med*. 2014;371:2499-2509.

11. Feinberg AP. The key role of epigenetics in human disease prevention and mitigation. *N Engl J Med*. 2018;378:1323-1334.
12. Gao A, Guo M. Epigenetic based synthetic lethal strategies in human cancers. *Biomark Res*. 2020;8.
13. Bryant HE, Schultz N, Thomas HD, et al. Specific killing of BRCA2-deficient tumours with inhibitors of poly(ADP-ribose) polymerase. *Nature*. 2005;434:913-917.
14. Tumor angiogenesis vascular growth and survival.pdf.
15. Hipfner DR, Cohen SM. Connecting proliferation and apoptosis in development and disease. *Nat Rev Mol Cell Biol*. 2004;5:805-815.
16. Huang EJ, Reichardt LF. Neurotrophins: roles in neuronal development and function. *Annu Rev Neurosci*. 2001;24:677-736.
17. Putz U, Harwell C, Nedivi E. Soluble CPG15 expressed during early development rescues cortical progenitors from apoptosis. *Nat Neurosci*. 2005;8:322-331.
18. Yao JJ, Gao X-F, Chow C-W, Zhan X-Q, Hu C-L, Mei Y-A. Neuritin activates insulin receptor pathway to up-regulate Kv4.2-mediated transient outward K+ current in rat cerebellar granule neurons. *J Biol Chem*. 2012;287:41534-41545.
19. Yao JJ, Zhao QR, Liu DD, Chow CW, Mei YA. Neuritin Up-regulates Kv4.2 alpha-subunit of potassium channel expression and affects neuronal excitability by regulating the calcium-calcineurin-NFATc4 signaling pathway. *J Biol Chem*. 2016;291:17369-17381.
20. Lamm N, Rogers S, Cesare AJ. The mTOR pathway: implications for DNA replication. *Prog Biophys Mol Biol*. 2019;147:17-25.
21. The Neurotrophin Neuritin1 cpg15 is involved in m Source Oncotarget 2016 Nov[PMIDT27901477].pdf.
22. Yuan M, Li Y, Zhong C, *et al*. Overexpression of neuritin in gastric cancer. *Oncol Lett*. 2015;10:3832-3836.
23. Zhang L, Zhao Y, Wang C-G, *et al*. Neuritin expression and its relation with proliferation, apoptosis, and angiogenesis in human astrocytoma. *Med Oncol*. 2010;28:907-912.
24. Dong H, Luo X, Niu Y, *et al*. Neuritin 1 expression in human normal tissues and its association with various human cancers. *Int J Clin Exp Pathol*. 2018;11:1956-1964.
25. Kang H-S. Differential methylation hybridization profiling identifies involvement of STAT1-mediated pathways in breast cancer. *Int J Oncol*. 2011;39:955-963.
26. Parker BS, Argani P, Cook BP, *et al*. Alterations in vascular gene expression in invasive breast carcinoma. *Can Res*. 2004;64:7857-7866.
27. Vincent A, Omura N, Hong S-M, *et al*. Genome-wide analysis of promoter methylation associated with gene expression profile in pancreatic adenocarcinoma. *Clin Cancer Res*. 2011;17:4341-4354.
28. Wu T-I, Huang R-L, Su P-H, Mao S-P, Wu C-H, Lai H-C. Ovarian cancer detection by DNA methylation in cervical scrapings. *Clin Epigenetics*. 2019;11:166-177.
29. Cao B, Yang Y, Pan Y, *et al*. Epigenetic silencing of CXCL14 induced colorectal cancer migration and invasion. *Discov Med*. 2013;16:137-147.
30. Herman JG, Graff JR, Myohanen S, Nelkin BD, Baylin SB. Methylation-specific PCR: a novel PCR assay for methylation status of CpG islands. *Proc Natl Acad Sci USA*. 1996;93:9821-9826.
31. Jia Y, Yang Y, Zhan Q, *et al*. Inhibition of SOX17 by microRNA 141 and methylation activates the WNT signaling pathway in esophageal cancer. *J Mol Diagn*. 2012;14:577-585.
32. Dong Y, Cao B, Zhang M, *et al*. Epigenetic silencing of NKD2, a major component of Wnt signaling, promotes breast cancer growth. *Oncotarget*. 2015;6(26):22126-22138.
33. Yu Y, Yan W, Liu X, *et al*. DACT2 is frequently methylated in human gastric cancer and methylation of DACT2 activated Wnt signaling. *Am J Cancer Res*. 2014;4:710-724.
34. Jia Y, Yang Y, Brock MV, *et al*. Methylation of TFPI-2 is an early event of esophageal carcinogenesis. *Epigenomics*. 2012;4:135-146.
35. Yan W, Kongming WU, Herman JG, *et al*. Epigenetic regulation of DACH1, a novel Wnt signaling component in colorectal cancer. *Epigenetics*. 2013;8:1373-1383.
36. Hou H, Zhang Y, Huang Y, *et al*. Inhibitors of phosphatidylinositol 3′-kinases promote mitotic cell death in HeLa cells. *PLoS One*. 2012;7(4):e35665.
37. Juvekar A, Hu H, Yadegarynia S, *et al*. Phosphoinositide 3-kinase inhibitors induce DNA damage through nucleoside depletion. *PNAS*. 2016;113:E4338-E4347.
38. Huang T-T, Brill E, Nair JR, *et al*. Targeting the PI3K/mTOR pathway augments CHK1 inhibitor-induced replication stress and antitumor activity in high-grade serous ovarian cancer. *Can Res*. 2020;80:5380-5392.
39. Chopra SS, Jenney A, Palmer A, *et al*. Torin2 exploits replication and checkpoint vulnerabilities to cause death of PI3K-activated triple-negative breast cancer cells. *Cell Systems*. 2020;10:66-81.e11.
40. Dutton SJ, Ferry DR, Blazeby JM, *et al*. Gefitinib for oesophageal cancer progressing after chemotherapy (COG): a phase 3, multicentre, double-blind, placebo-controlled randomised trial. *Lancet Oncol*. 2014;15:894-904.
41. Janmaat ML, Gallegos-Ruiz MI, Rodriguez JA, *et al*. Predictive factors for outcome in a phase II study of gefitinib in 2nd-line treatment of advanced esophageal cancer patients. *J Clin Oncol*. 2006;24:1612-1619.
42. Yang J, Liu X, Cao S, *et al*. Understanding esophageal cancer: the challenges and opportunities for the next decade. *Front Oncol*. 2020;10(10):1727. https://doi.org/10.3389/fonc.2020.01727
43. Guo MZ, Liu S, Lu F. Gefitinib-sensitizing mutations in esophageal carcinoma. *N Engl J Med*. 2006;354:2193-2194.
44. Guo MZ, Liu S, Herman JG, Zhuang H, Fengmin LU. Gefitinib-sensitizing mutation in esophageal carcinoma cell line. *Cancer Biol Ther*. 2006;5(2):152-155.
45. Song Y, Li L, Ou Y, *et al*. Identification of genomic alterations in oesophageal squamous cell cancer. *Nature*. 2014;509:91-95.
46. Guo M, Ren J, House MG, Qi YU, Brock MV, Herman JG. Accumulation of promoter methylation suggests epigenetic progression in squamous cell carcinoma of the esophagus. *Clin Cancer Res*. 2006;12:4515-4522.
47. Guo M, Peng Y, Gao A, Du C, Herman JG. Epigenetic heterogeneity in cancer. *Biomark Res*. 2019;7:23. https://doi.org/10.1186/s40364-019-0174-y
48. Pfister SX, Ashworth A. Marked for death: targeting epigenetic changes in cancer. *Nat Rev Drug Discovery*. 2017;16:241-263.
49. Guo M, Ren J, Brock MV, Herman JG, Carraway HE. Promoter methylation of HIN 1 in the progression of ESCC. *Epigenetics*. 2008;3(6):336-341.
50. Jia Y, Yang Y, Zhan Q, *et al*. Inhibition of SOX17 by MicroRNA 141 and methylation activates the WNT signaling pathway in esophageal cancer. *J Mol Diagn*. 2012;14:577-585.
51. He T, Zhang M, Zheng R, *et al*. Methylation of SLFN11 is a marker of poor prognosis and cisplatin resistance in colorectal cancer. *Epigenomics*. 2017;9(6):849-862.
52. Cao B, Yang W, Jin Y, *et al*. Silencing NKD2 by promoter region hypermethylation promotes esophageal cancer progression by activating Wnt signaling. *J Thorac Oncol*. 2016;11:1912-1926.
53. Hou J, Liao L-D, Xie Y-M, *et al*. DACT2 is a candidate tumor suppressor and prognostic marker in esophageal squamous cell carcinoma. *Cancer Prev Res*. 2013;6:791-800.
54. Huang T-T, Lampert EJ, Coots C, Lee J-M. Targeting the PI3K pathway and DNA damage response as a therapeutic strategy in ovarian cancer. *Cancer Treat Rev*. 2020;86:102021.

How to cite this article: Du W, Gao A, Herman JG, et al. Methylation of NRN1 is a novel synthetic lethal marker of PI3K-Akt-mTOR and ATR inhibitors in esophageal cancer. *Cancer Sci*. 2021;112:2870–2883. https://doi.org/10.1111/cas.14917